

A sensor for dynamic tactile information with applications in human-robot interaction and object exploration

Peer A. Schmidt ^a, Eric Maël ^b, and Rolf P. Würtz ^{c,*}

^a*Hilti Corporation, Feldkircherstrasse 100, FL-9494 Schaan, Liechtenstein*

^b*Precision Robotics GmbH, Greifswalderstr. 212-213, D-10405 Berlin, Germany*

^c*Institut für Neuroinformatik, Ruhr-Universität, D-44780 Bochum, Germany*

Abstract

We present a novel tactile sensor, which is applied for dextrous grasping with a simple robot gripper. The hardware novelty consists of an array of capacitive sensors, which couple to the object by means of little brushes of fibers. These sensor elements are very sensitive (with a threshold of about 5 mN) but robust enough not to be damaged during grasping. They yield two types of dynamical tactile information corresponding roughly to two types of tactile sensors in the human skin. The complete sensor consists of a foil-based static force sensor, which yields the total force and the center of the two-dimensional force distribution and is surrounded by an array of the dynamical sensor elements. One such sensor has been mounted on each of the two gripper jaws of our humanoid robot and equipped with the necessary read-out electronics and a CAN bus interface. We describe applications to guiding a robot arm on a desired trajectory with negligible force, reflective grip improvement, and tactile exploration of objects to create a shape representation and find stable grips, which are applied autonomously on the basis of visual recognition.

Key words: tactile sensor, dextrous manipulation, trajectory teaching, dynamic tactile sensor, humanoid robot, object exploration, autonomous grasping.

* Corresponding author

Email addresses: peer.schmidt@hilti.com (Peer A. Schmidt),

mael@precision-robotics.com (Eric Maël),

rolf.wuertz@neuroinformatik.rub.de (Rolf P. Würtz).

URL: <http://www.neuroinformatik.rub.de/PEOPLE/rolf/> (Rolf P. Würtz).

1 Introduction

Dextrous grasping with a humanoid has to face the problem that the cameras are located at a considerable distance from where the actual manipulation takes place. Consequently, three-dimensional visual analysis has significant inaccuracy. It can be reduced if cameras are mounted on the manipulator itself, but such a setup can hardly be called humanoid.

Starting from these problems the idea arose to live with the visual inaccuracies and do fine tuning during grasping by means of *tactile* sensing. To that end the sensing devices should have high sensitivity and high spatial resolution.

Another important purpose, which is not served well by available sensors, is to detect contact early and with as little force as possible in order to minimize the probability of damage to both the robot and the objects in the environment. Vision is not suited for this, because the actual contact points need not be visible and analysis of three-dimensional scenes is, at the current state of the art, by far not accurate enough.

1.1 *Tactile sensors in the human skin*

As the human tactile sense is very accurate and sensitive, it is worthwhile to take a brief look at the biological hardware. Glabrous human skin contains four different types of tactile sensors; a list of their properties is given in Tab. 1. The most important distinction between the sensor types is between *static* and *dynamic*, in the sense that dynamic sensors do not react to (temporally) constant pressure. The static *Merkel* and *Ruffini corpuscles* react to static pressure on the skin. *Meissner cells*, the first dynamic type, roughly measure the speed of skin indentation, and *Pacini corpuscles* preferably react to vibrations or changes of indentation speed. Their characteristic is mainly due to an onion-like sheet, which effectively applies a mechanical high-pass filter to the indentation signal. In hairy skin there are similar tactile sensors, but the Merkel receptors are replaced by *dome* or *Pinkus-Iggo corpuscles*, *Meissner corpuscles* are functionally replaced by *hair follicle cells*.

The dynamic sensors are of special importance for actively checking surface properties. The rough surface of, e.g., a coin cannot be distinguished from a perfectly flat one by applying static pressure with a finger, while slightly rubbing a surface reveals that information immediately. This is one example for the necessity of active tactile sensing for object analysis. Another one is the exploration of object shape and the improvement of imperfect grips. Also, unexpected contact is best determined by dynamic sensors, because in the beginning of the contact the temporal derivatives are already high while the

Type	Merkel	Ruffini	Meissner	Pacini
Number	25%	19%	43%	13%
Adaptivity	Slow	Slow	Fast	Fast
Response to indentation $S(t)$ proportional to	$S, \frac{ds}{dt}$	S	$\frac{ds}{dt}$	$\frac{d^2s}{dt^2}$
Response to constant indentation	Yes	Yes	No	No
Location	Superficial	Deep	Superficial	Deep
Receptive field	Small	Large	Small	Large
Innervation density	High, variable	Low, constant	High, variable	Low, constant

Table 1

Tactile sensors in the human skin and their characteristics.

indentation is still small.

On the other hand, static pressure sensors are required for, e.g., force feedback during grasping. Consequently, our needs would best be met by a combination of dynamic and static sensing elements in an integrated sensor module similar to a patch of skin.

1.2 Technical tactile sensors

In this section we give a brief review of technical tactile sensors. The following basic sensing principles are commonly in use.

Capacitive sensors consist of a plate capacitor. Forces on these sensors either modify the plates' distance or the effective area by shifting their relative position. They can be made very small, which allows the construction of dense sensor arrays, and also allow dynamic measurements. Their stray capacity is a major problem, because it can reach the order of magnitude of the capacity to be measured. For examples see [1].

Piezoelectrical sensors contain a piezoelectrical substance, which creates a measurable charge under force or deformation. They are restricted to dynamic measurements and particularly suited for measuring vibrations [2].

Inductive sensors measure the changing *self-inductance* caused by a change of geometry or magnetic coupling. Usually, the size of the sensors makes this technology more appropriate for force/torque sensors than for tactile ones. The *linear variable differential transformer (LVDT)* by Schaevitz Engineering is widely used [3]. A newer version suited for the use in elastic

finger tips is described in [4].

Optoelectrical sensors usually consist of a light source, a modulatory medium, a transmission medium and a photo detector. Pressure leads to a change of *light intensity* in the transmission medium, which can be registered in the detector.

Piezoresistive sensors change their *resistance* under pressure. They are attractive because measuring resistance requires little electronics. Beside metallic or semiconductor *extensometers* and *conductive elastomers* so called *force sensing resistors (FSR)* are widely used. A semiconductive polymer ink, which reduces its resistance from 10 M Ω down to 1 k Ω under pressure, is applied to a plastic foil.

The use of these basic techniques for tactile sensing is reviewed in [5,6].

2 The sensor hardware

In the following we describe the construction of our combined tactile sensor.

2.1 Static sensor

The static part of the sensor is built following Liu et al. [7]. On our prototype, it measures force in the range between 50mN and 10N. It consists of a piezoresistive foil sensor, which is based on a foil coated with a semi-conductive ink. This foil changes its resistance logarithmically with pressure. It is produced by Interlink Electronics, who sell it under the label force-sensing-resistor (FSR) and also hold the patent on this technique. To measure amount and position of force applied to the foil, we placed another foil with two electrodes under the piezoresistive foil. The electrodes consist of nested parallel contact fingers. The contact fingers of the first electrode are directly connected to each other, and the ones of the second electrode are connected via a linear potentiometer. Measuring the resistance between the foils (the overall resistance of the linear-potentiometer is negligible) yields the force information. Applying a voltage to the edges of the potentiometer of the second electrode and measuring the voltage at the first electrode provides the information about the position of the force in one direction. In order to get the full 2-D coordinates two such systems are put on top of each other.

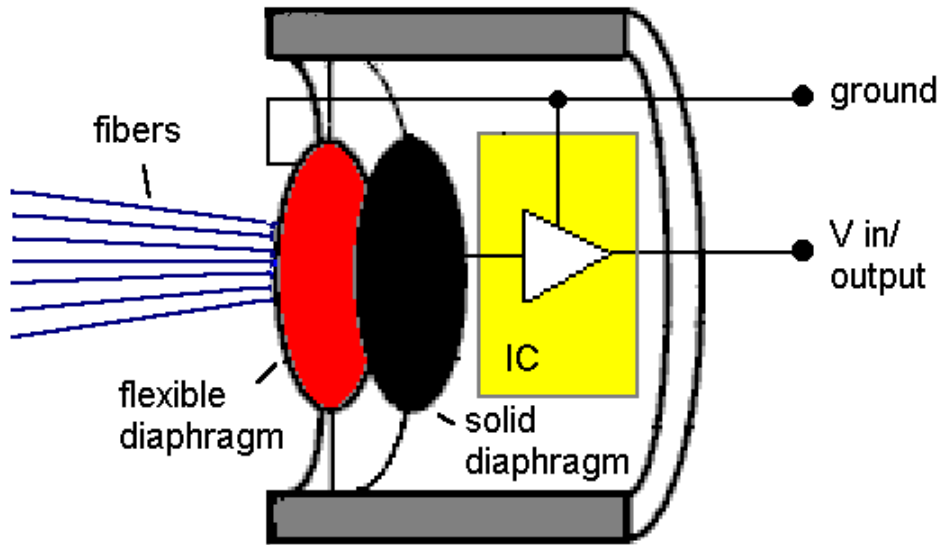


Fig. 1. Schema of a dynamic sensor element with fibers, capacitor and IC.

2.2 *Dynamic sensor element*

In order to allow for dense sensor arrays we have decided to build a capacitive dynamic sensor. The receptive part of the sensor consists of two round capacitor membranes. For our prototype they have been taken from a condenser microphone by Teisco. The plates have a radius of 2mm, a resting distance of $40\ \mu\text{m}$, and a capacitance of 2.8 pF. The microphones have an IC attached to the fixed membrane, which basically serves as a field effect transistor to reduce the stray capacity (see Fig. 1). It also recharges the capacitor plates after a distance change with a time constant of about 300 ms.

The major problem we had to solve was the coupling of the capacitor to the object. Usually, the sensing element is covered with some elastic material, which leads to spatial low-pass filtering of the contact information and also requires relatively high forces for a deformation large enough to be registered by the sensor.

These disadvantages could be resolved by a novel mechanical transduction technique. A little brush of fibers is attached to the flexible membrane with a silicon resin. Upon contact with the object these fibers transmit the force to the capacitor and change the plate distance.

By appropriate choices for fibers, membrane and resin, the time course of the capacitor charge reflects the approaching speed of the actuator to an object. The number of fibers attached to a capacitor is a parameter that can be adapted to the desired application. In our prototype we have used some 30

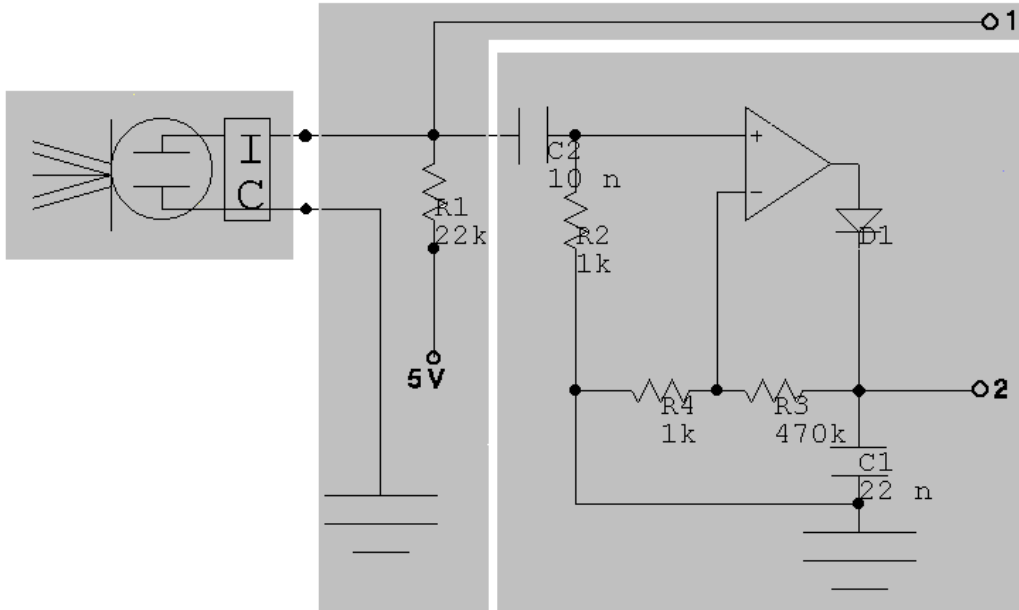


Fig. 2. Circuitry for a dynamic sensor element. The left part is a schematic representation of the element, the middle part extracts the raw (speed) signal at pin 1, and the right part is a combined high-pass filter and a sample/hold/forget circuit that yields the vibration signal at pin 2.

fibers per element.

Due to the flexibility of the fibers, this method is not suitable for the transmission of static forces but ideal for sensing vibrations and detecting contact. For the latter, only very small forces (less than 10 mN) need to be exerted on the object.

Additional to the raw signal, which is useful for the detection of contact and speed of approach, we have applied an analogue high-pass filter followed by a “sample/hold/forget” circuit to measure vibrations. The latter is a standard sample/hold circuit which discharges with a time constant of 10 ms. These two signals, which we will call the *speed signal* and the *vibration signal*, roughly correspond to the information from Meissner and Pacinian corpuscles, respectively. The complete circuitry for a dynamic element is shown in Fig. 2.

2.3 Combined sensor

A combined sensor consists of two static elements (for x- and y- direction) surrounded by 16 dynamic sensor elements. One of them is mounted on each jaw of a two-jaw gripper. Each static element yields a position and a force signal, the latter is redundant for the two directions. Each dynamic element

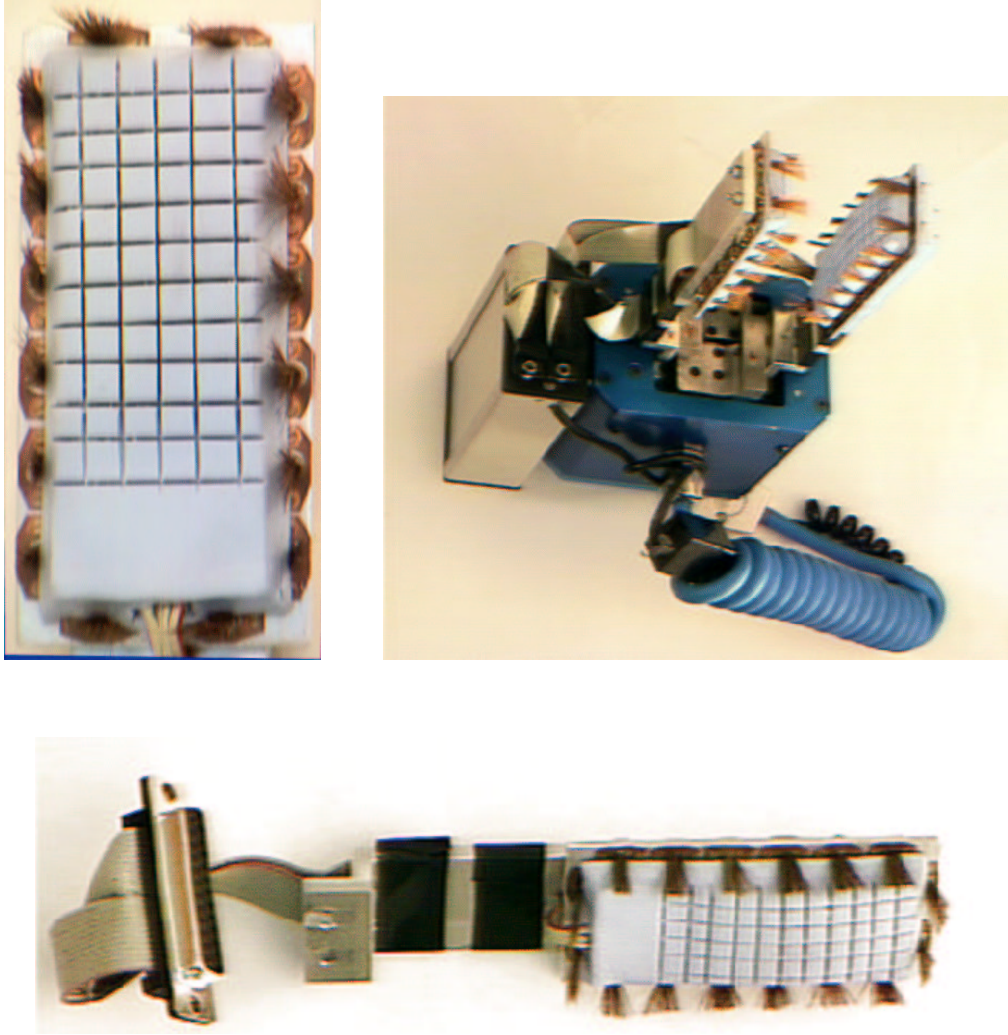
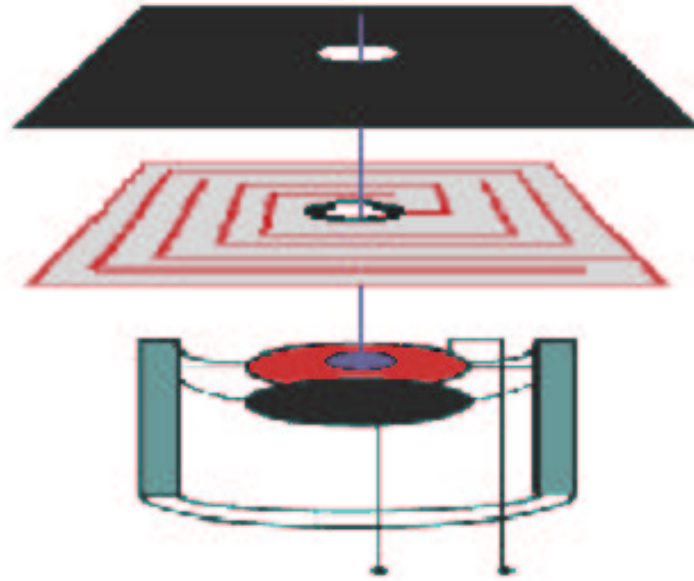


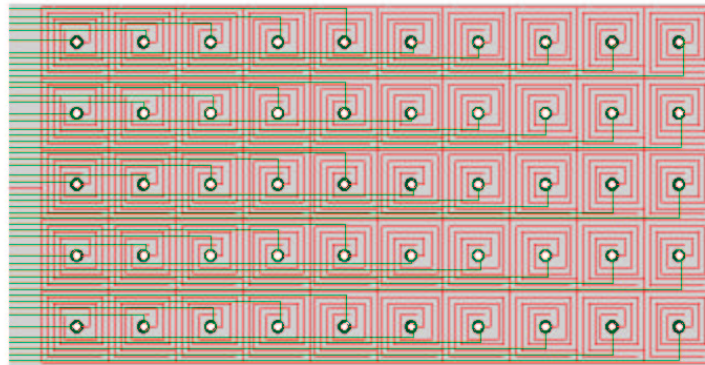
Fig. 3. Complete sensor. The static part is located under the central blue polymer layer, the dynamic elements are positioned on the rim. One of these combined sensors is mounted on each jaw of the gripper, and the grey box attached to the gripper body contains the processing electronics including the CAN bus controller.

produces a speed and a vibration signal, which results in a total of 72 signals for a whole two-jaw gripper. The electronics for a whole gripper is placed into a box attached to the gripper body (see Fig. 3).

Later, four additional dynamic sensors have been added to the tips of the gripper jaws in order to detect contact to the table during grasping. Generally, the setup can be adapted very flexibly to special needs; a layout for a more skin-like sensor is shown in Fig. 4, where a combination of static FSR sensor and dynamic sensor can be repeated and potentially strongly miniaturized to provide a sensitive skin with high spatial resolution. Such sensing devices can be organized as dense sensor networks [8]. With a different technology, the resolution of the papillary ridges on human skin has been reached [9].



a)



b)

Fig. 4. Schematic layout of a skinlike sensor. **a)** The top layer consists of pressure sensitive FSR foil, the middle one is the electrode layer, and the bottom layer contains a dynamic sensor with a single hair or small brush, which connects to the surface via a small hole in the upper layers. These elements can be repeated like shown in **b)**.

2.4 Processing of the sensor signals

The analogue signals from both types of sensor elements are digitized and processed on a C515C microcontroller by Siemens. This microcontroller contains an A/D converter with eight channels, therefore an analogue circuit has been constructed to multiplex the signals from the gripper before digitization. For the 72 signals in the current setup 4 of the channels have been used leaving some potential for further extensions, e.g., for the addition of torque sensors in the gripper joint.

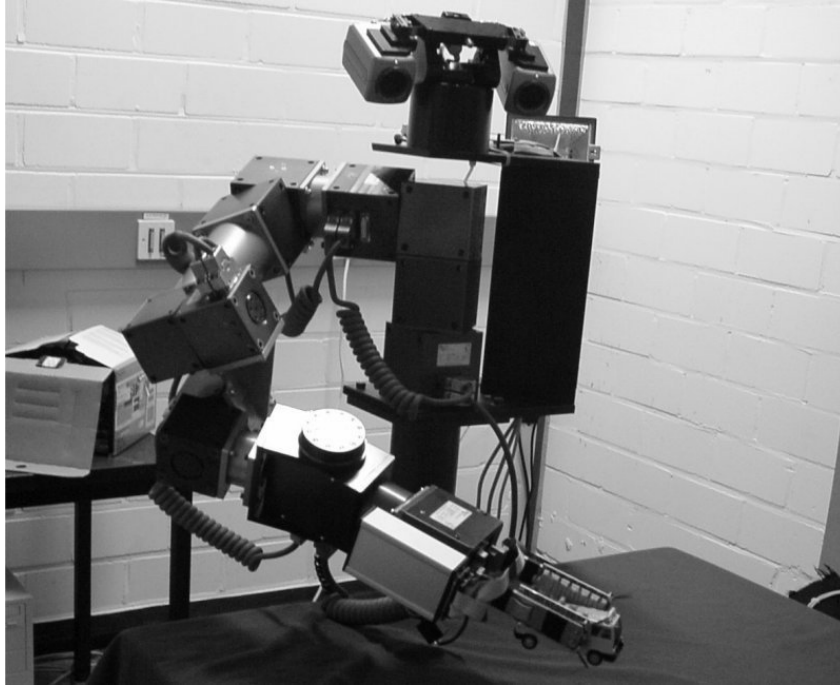


Fig. 5. The robot platform with 3 DoF stereo camera head, 7 DoF manipulator, and tactile sensors.

The C515C also contains a CAN bus controller, which made it possible to address the sensor module just like any of the robot modules making up the arm.

Patents on this sensor technique have been granted in Europe and the US [10,11], the Japanese application is pending [12]. Full details of the construction of our prototype can be found in [13].

2.5 The robot

The following experiments have been carried out on our humanoid robot platform, which is described in detail in [14]. As depicted in Fig. 5 it consists of the following components:

- One modular robot arm with seven degrees of freedom (DoF), kinematics similar to a human arm, and a parallel jaw gripper;
- a dual stereo camera head with three DoF (pan, tilt, and vergence) and a stereo basis of 30 cm for two camera pairs with different fields of view (horizontally 56° with color and 90° monochrome, respectively);
- a computer network composed of four Pentium PCs under Linux and a Sun UltraSPARC II workstation under Solaris.

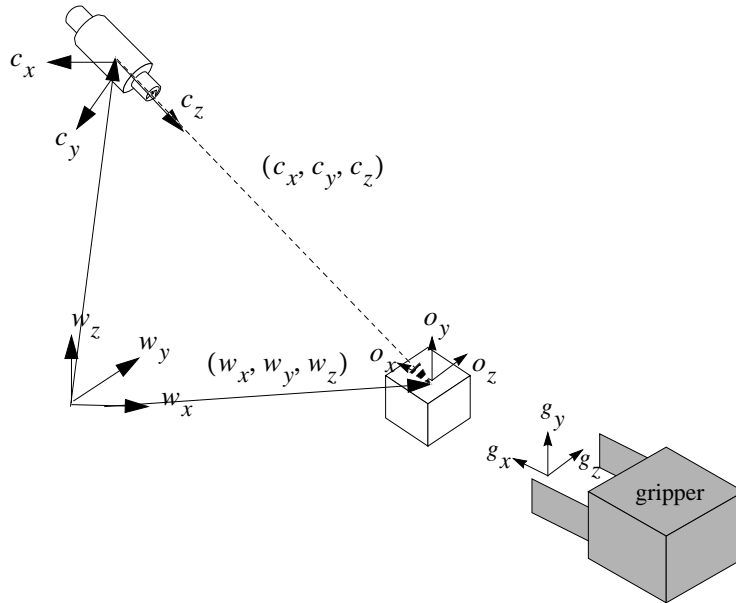


Fig. 6. Coordinate systems used.

One of the PCs is reserved for control of the robot arm, a second performs image acquisition through two color frame grabber boards, controls the camera head, and does some real-time image processing. The processors are networked with FastEthernet to achieve sufficient throughput and low latencies.

3 Applications

3.1 Sensor properties

In the following we present experiments to probe the properties of the sensor. These experiments suggest that the *speed of approach* of an object can be estimated from the raw (original) sensor signals, while vibrations and situations like sliding objects are best detected using the high-pass filtered vibration signal.

In the first experiment, a sensor element has been rapidly brought into contact with an object and not been removed. The time course of both signals is shown in Fig. 7 a). There are hardly any vibrations, but the speed signal reaches its maximum a few milliseconds after contact. The further course shows the adaptation, which restores the original voltage after 300ms.

In the second experiment, shown in Fig. 7 b), an object approached a sensing element with different speeds and was stopped suddenly. The resulting vibrations reflect the vibration of the whole measuring apparatus and are su-

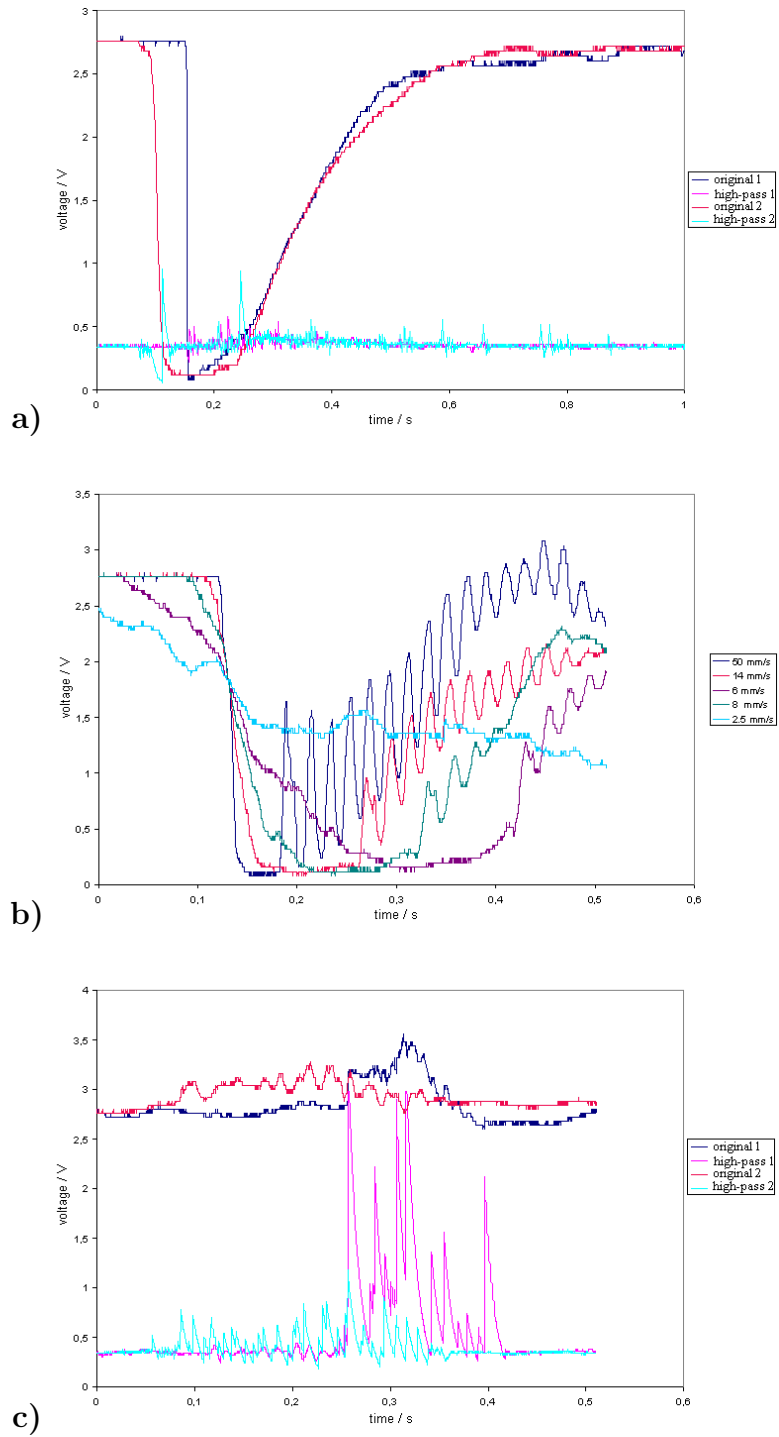


Fig. 7. Raw (original) and high-pass filtered sensor signals during approach and slip. **a)** Fast approach of an object. After the approach the object has not been removed, which reveals the adaptivity of the sensor. **b)** Original signal at different approach speeds. Contact took place at the moment of strong voltage decrease (outside the diagram for 2.5 mm/s). Stopping the piston leads to vibrations in the sensor mount, which are superimposed on the adaptation. **c)** Signals at beginning slip. Slip can be nicely detected in the high-pass filtered vibration signal.

perimposed on the adaptation. In the early phase it can be seen that the slope of the signal is strongly correlated with the speed of approach.

The third experiment starts with an object held with a stable grasp between the gripper jaws. Then the closing force is reduced until the object begins to slide. Fig. 7 c) shows two different time courses. It can be seen that the speed signal is hardly influenced by sliding, which in turn can be clearly detected in the vibration signal.

Other sensors used for slip detection [15,16] rely on relatively high forces between sensor and object. This allows to detect the start of slipping in a very short time interval. In our case, a slipping object causes vibrations in the fibers, which are sustained as long as there is contact.

In order to assess the sensor properties quantitatively, we have measured the reaction to sine-signals of variable frequency. To that end, a dynamic sensor element has been put into contact with the membrane of a speaker vibrating at the respective frequency. Sensor gain is defined as the ratio of the signal voltage to the noise level at zero vibration amplitude in dB. The results are shown in Fig. 8 a). The dependence of sensor gain on the logarithm of the amplitude is about linear for 10Hz and 100Hz, which means that the unfiltered sensor signal is a good measure of the input. For these measurements, the actual amplitude of the membrane has been verified by measuring contact with a micrometer gauge.

Hysteresis is very low, because there is no viscous polymer, and the fibers return to their resting state very quickly. Fig. 8 a) shows that the responses at 10Hz and 100Hz are the same, and it can be concluded that a remaining deformation decays in less than 10ms. For compliant sensors with polymer coating this time is on the order of 1 second [17].

The dynamic range of the sensors has been determined by applying sine-signals of constant power (i.e. decreasing amplitude) over the whole frequency spectrum and measuring the sensor gain. In this experiment we have not measured the amplitude of the speaker as a function of frequency, so the curve in Fig. 8 b) is a superposition of the speaker and sensor characteristics. However, it can be seen that useful measurements are possible up to 35kHz.

It should be mentioned that these properties depend mainly on the mechanical properties (length, stiffness, number per sensor) of the fibers involved and can be easily adjusted according to the needs of the application.

As we have only built a few prototypes, we have not made systematic experiments on the durability of the sensors. The prototype on the robot has been in regular use for about 5 years, for an estimated total of 400 hours. After that, the sensor elements were still working properly without recalibration.

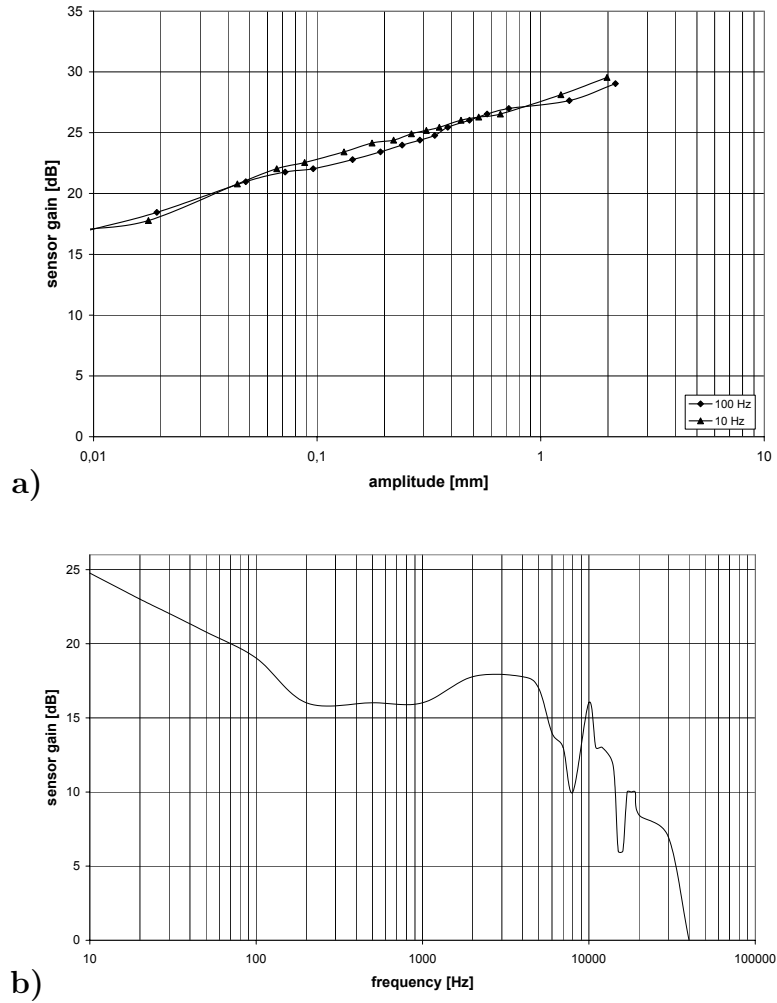


Fig. 8. Response of a dynamic sensor element to sine vibrations. **a)** At 10Hz and 100Hz, the sensor gain has about the same dependence on amplitude. **b)** The dynamic range, where measurements are possible, goes up to about 35kHz.

Regular use includes manipulation of objects and guidance by hand, which leads to rough treatment and some staining of the sensors. The weakest part seems to be the resin which attaches the fibers to the capacitor, as some of them detached in the meantime. This suggests that the technique could well be useful for industrial use, while product development would have to apply some optimization of the materials.

3.2 Manual guidance of the robot arm

Teaching by demonstration has become an important and efficient way to instruct robots [18]. One aspect is moving actuators on a desired trajectory and having the robot learn the trajectory for later autonomous execution.

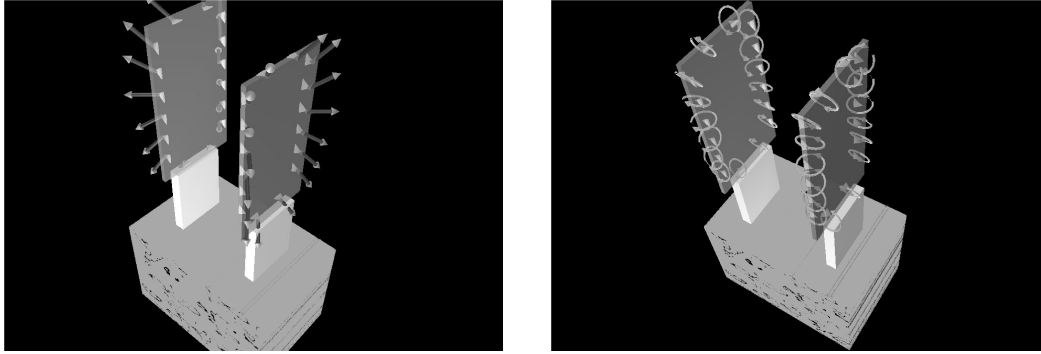


Fig. 9. The translational (left) and rotational (right) vector fields of the inner hair sensors. The translational one is radial in order to center the gripper around an object, and the rotational one is circular in order to orient the gripper parallel to the object surface.

Tactile sensing is useful for that [19,20,21]. Because of the small forces required the type of tactile sensors described here is particularly suited for this task. To demonstrate this, we have implemented a method for guiding the robot arm manually on a desired trajectory, the *Robot-Guidance-Client*. The state of the gripper in the 3D workspace is described by 7 DoF, namely 3 for translation, 3 for orientation and 1 for opening and closing the jaws (The redundant DoF in the arm is not counted here). We have implemented a control strategy that attempts to maximize the number of contact points. This way, 5 of these DoF can be controlled, with the exception of wrist pitch (the rotation around the axis between the gripper tips) and the gripper opening, which is adjusted to always fit the object used for guidance.

The control strategy is as follows. The speed signal from each sensor is binarized with a suitable threshold and triggers a predefined reflex movement, which is represented by a translational and a rotational movement vector relative to the gripper. The translation vector moves the contact position towards a target position, e.g., the center between both gripper jaws. This results in a radial vector field for the translation, where each direction is given by a vector pointing from the target position towards the sensor position. The rotation vector turns the gripper such as to maximize the number of sensor contacts, i.e., it attempts a parallel orientation of the gripper jaw to the hand's surface. Both vector fields are shown in Fig. 9. The opening width of the gripper is controlled to keep loose contact with the hand. In case of contact with both gripper jaws it receives a small opening signal, and in case of one-sided contact a small closing signal.

This control method can be used to guide the robot arm on a desired trajectory by putting a hand (or ideally an object with parallel surfaces like a book) between the jaws. If adjusted suitably, the movement components of each sensor element add up to a motion which minimizes the asymmetry of the

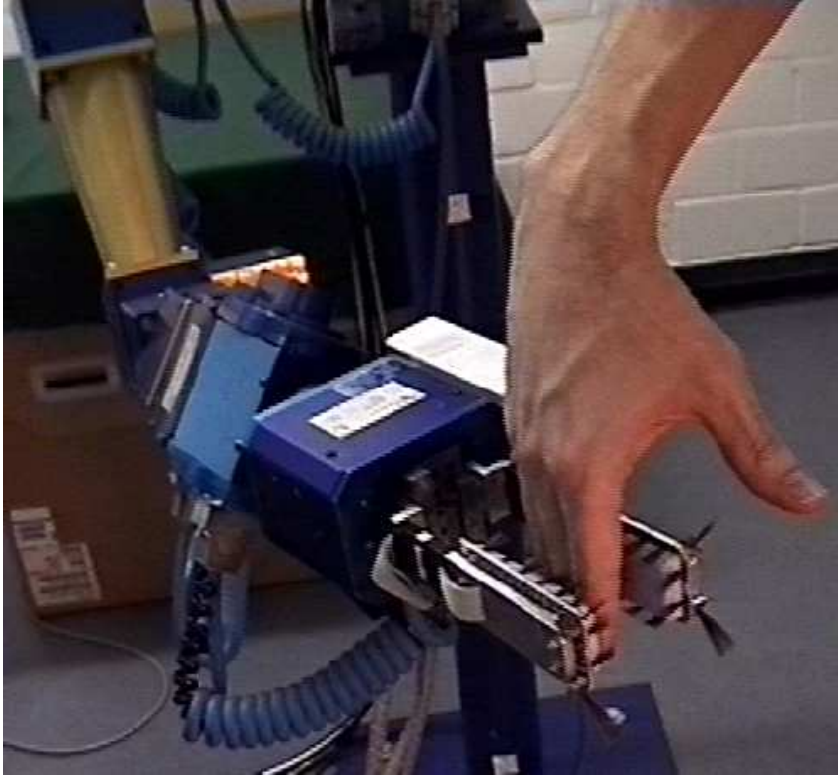


Fig. 10. Using the tactile sensors the robot arm can be guided on a desired trajectory with negligible force.

contact around the hand and thus follows the hand's movement through the configuration space (Fig. 10). Full details about the dynamics and the overall robot control can be found in [22].

3.3 Reflective grasping

Although fine-tuning of grips is mostly done with laser-range finders, there are several attempts to exploit tactile sensor information for this task, one recent example being [23]. We here describe the extension of the guidance module to a reflective grasping behavior.

When the gripper is in contact with a simple static object with parallel grasping surfaces, the running Robot-Guidance-Client will eventually converge to a situation with a symmetric contact distribution around the desired grasping position on each gripper jaw. This is assumed to be a good grasping position and the gripper is closed.

If we assume stationary objects, any contact of a tactile sensor element with the object yields the world coordinates of a point on the object surface. The collection of many surface points can then be turned into a 3D-representation

of the object. This can in turn be used to estimate stable grips on a pair of parallel surfaces of appropriate distance. To achieve this, the following behaviors have been implemented.

The Robot-Guidance-Client has been extended to a *Generic-Grip-Client*. It uses the same vector fields and dynamics but additionally contains drift terms, which add a slow rotation around the y-axis at the tool-center point, and slow translations in x- and y-directions (see figure 6 for the coordinate systems used). Each of these drifts can have positive or negative direction, and the signs are changed when all sensors lose contact to the object. The Generic-Grip-Client can also switch to a *tipping mode*, in which only the long sensors on the tips of the jaws influence the behavior, and a larger region of space can be explored rapidly. This module is enough to grasp an object, but for exploration of complicated 3D shapes more complicated behavior is required.

3.4 Estimation of complete object shape to find stable grips

An object is explored by bringing the gripper into contact and starting a Generic-Grip-Client. During its course, all contact points are recorded by the known 3D-position of each sensor during contact. The point cloud is extended by a new point if its minimal distance to the cloud exceeds a threshold s_{\min} . When the number of points stagnates over a longer period of time it is assumed that the locally accessible part of the object is explored. Then the convex hull of the current point cloud is calculated, together with a list of its planar surface parts. This is done by the α -shape algorithm [24]. Those surface parts with an area exceeding a threshold are assumed to belong to unexplored object parts, and their centers are listed as future exploration targets. The surface part with a minimal number of points close to it is selected for exploration first, the arm is repositioned into a suitable position, and the Generic-Grip-Client continues with the exploration. Figure 11 shows the sequence of gripper positions required to explore the object. If an object is too large to be surrounded by the gripper, the Generic-Grip-Client can switch to its tipping mode. Exploration is repeated until plane surface parts of a size above threshold are exhausted.

The shape of the object must then be inferred from the point cloud. If it cannot be assumed that the object is convex, a good method to do this is to calculate the α -shape with a suitable α [24]. In our procedure, the value of α is chosen such that always one connected object results, which can still have unexplored holes. The convex hull is the limit of the α -shape with $\alpha \rightarrow \infty$.

This description of an object's surface is then analyzed to find a pair of sufficiently parallel and sufficiently plane surfaces for grasping. To that end, each

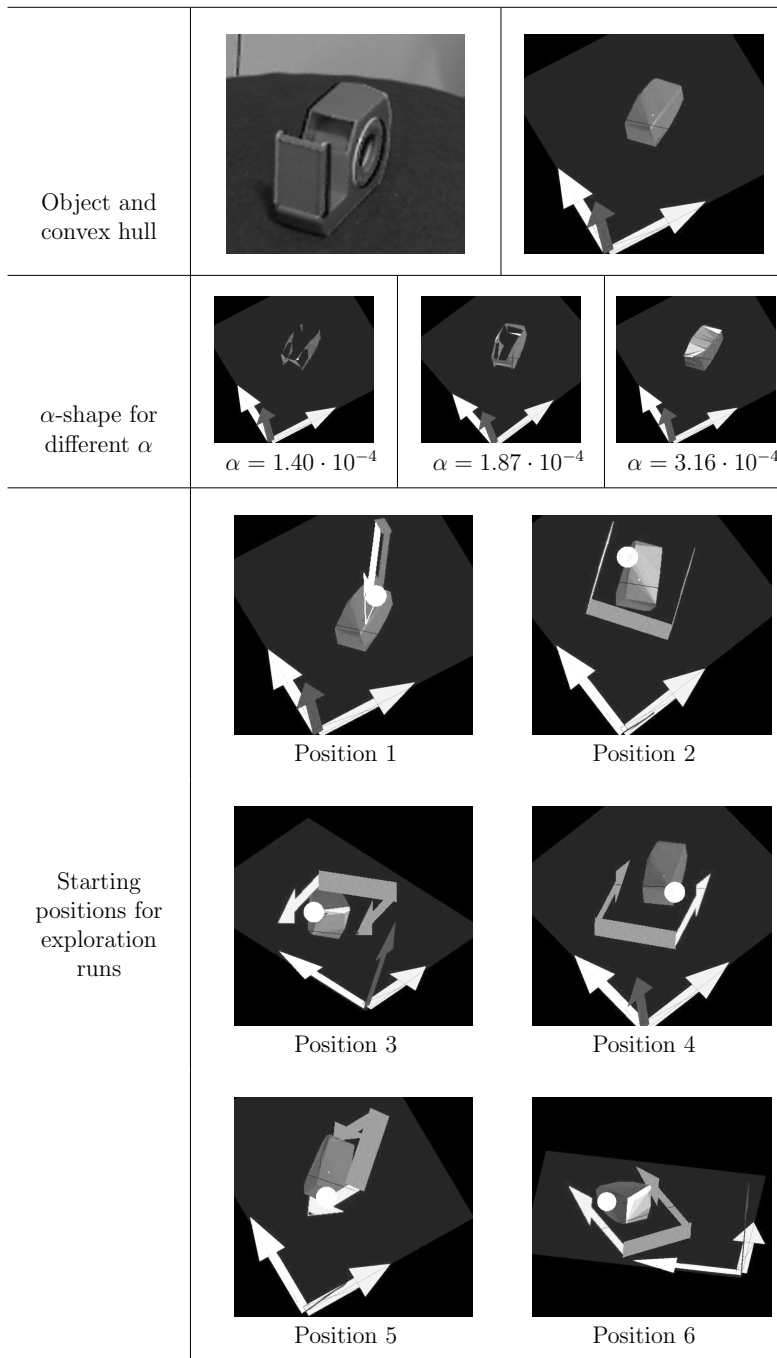


Fig. 11. Determining the starting positions for the next explorations of a partly known object (Tape). The α -shapes in the second row visualize the state of the point cloud. The next exploration positions are shown with the gripper as a parallel pair of arrows. An open gripper stands for normal exploration, a closed one for tipping mode. The bright dots represent the target positions for exploration. World coordinate axes are shown in the lower left corner.

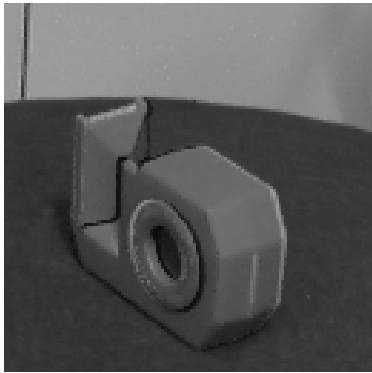
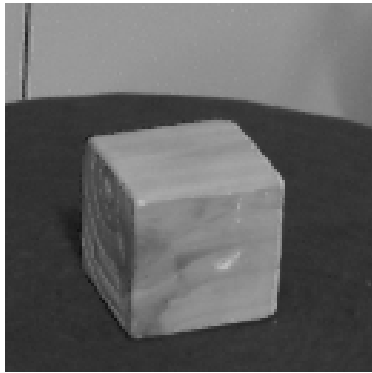
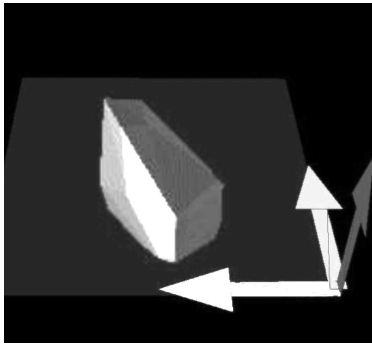
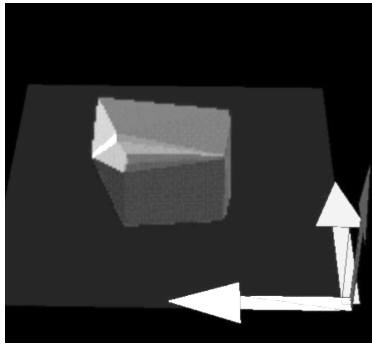
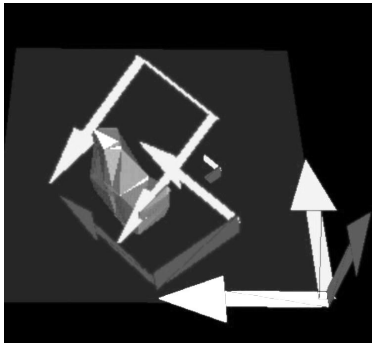
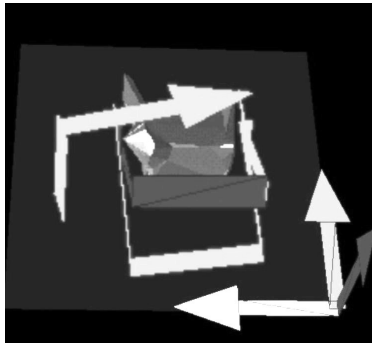
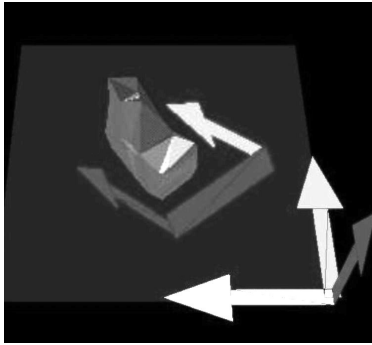
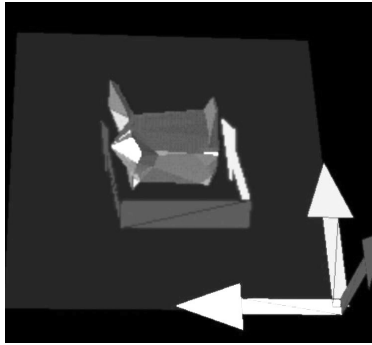
	tape	cube
Object aspect		
Convex hull		
α -shape with all grips		
Best grip		

Fig. 12. Convex hull and possible grips (tape and cube). World coordinate axes are shown in the lower left corner.

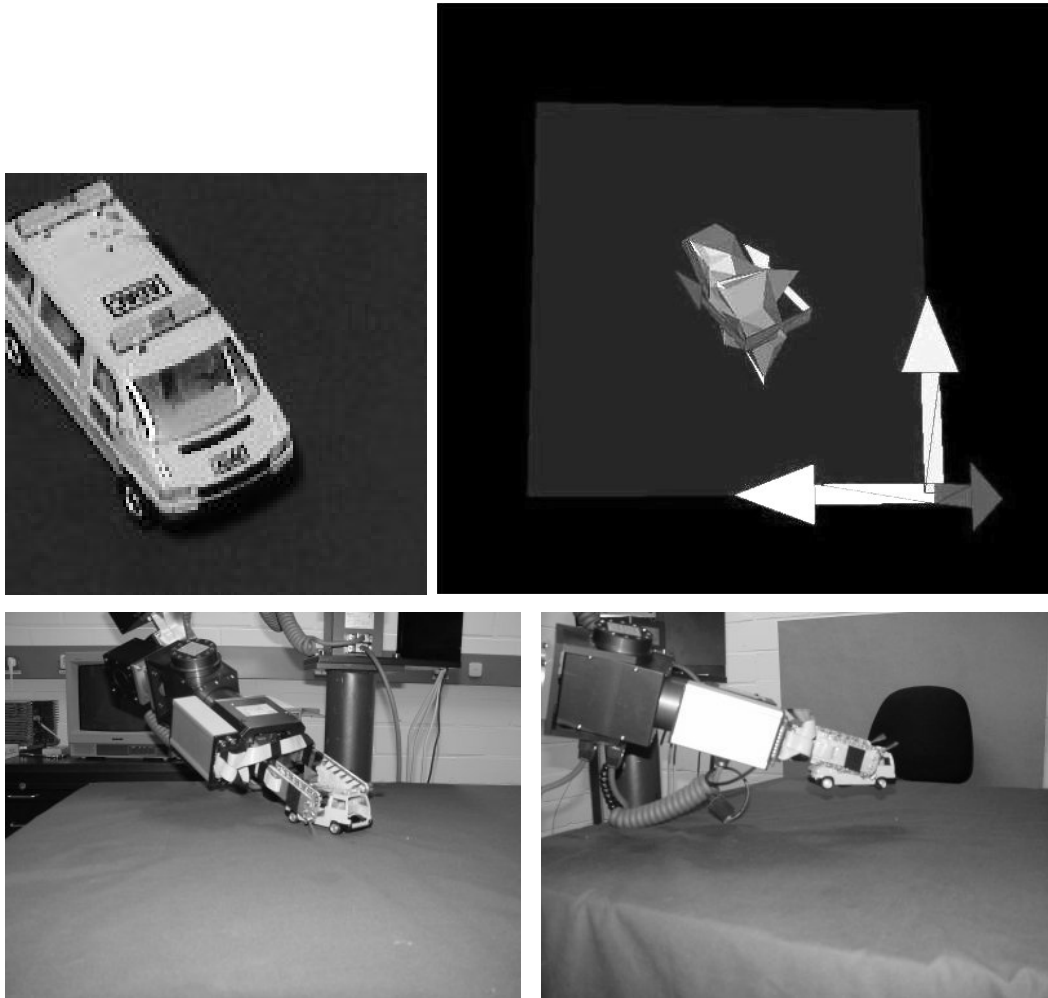


Fig. 13. Autonomous grasping of an object. Top: Camera image and shape representation rotated according to the recognized pose, with optimal grip. Bottom: Application of grip and lifting of the object.

surface element of the alpha-shape is extended by the points belonging to its neighboring surface element. The resulting point cloud is analyzed by Principal Component Analysis (PCA). This is iterated until the 3rd principal component exceeds a threshold, meaning that the resulting surface is not plane enough. The process is iterated with a new surface element, until all surface elements are assigned to a surface. From this set of surfaces, pairs of relatively parallel ones are selected, if their distance fits the gripper opening. A final criterion is that their angle to the table surface is not too small, because that would lead to difficulties in actually applying the grip.

This procedure, whose full details can be found in [25], yields a set of stable grips also for relatively complicated objects like the tape roll (see Fig. 12).

3.5 *Autonomous grasping of visually recognized objects*

A combination of a tactile and visual representation can be used to autonomously grasp known objects. Pose and identity of objects are estimated using a visual recognition system [26]. The object identity links to a previously created tactile shape representation, which is aligned to the actual situation by means of the pose angles. Then the most stable grip is selected and executed. A successful example is shown in Fig. 13. We have demonstrated this behavior for a set of five objects [25,27].

4 Discussion

We have equipped a two-jaw gripper with our combined sensor. The sensor technology we have developed, however, lends itself for arbitrary effector shapes and can certainly be used on the fingers of a robot hand. Especially the design described in Fig. 4 b) would probably be very well suited. The portion of space that a sensor element surveys can be controlled by modifying the number of fibers in a bundle and the length and material of the fibers themselves. Given automated production and moderate miniaturization the sensors we propose can be used to build a sensitive robot skin with relatively fine spatial resolution.

The most distinguishing feature of the new sensor type is the sensitivity. Forces as low as 5 mN can be detected, yet the sensors are not damaged when deformed by grips with forces high enough to apply stable grips to everyday objects.

We have shown that the two-jaw gripper equipped with these sensors is suited for refining grips attempted on the basis of visual information. Furthermore, we have presented a method for teaching trajectories with minimal force by touching only the fibers of the dynamic sensors.

We have presented a method to explore an object and create a purely tactile surface representation. Despite the low spatial resolution of our sensor prototype, this was detailed enough to identify surface pairs suited for stable grasping. Finally, the shape representation has been linked to visual recognition to allow autonomous grasping of known objects.

Acknowledgments

We are grateful to Jan Jockusch from the Technical University of Bielefeld and Liu Hong from the DLR in Oberpfaffenhofen for their help with the static sensors and for sharing their technical knowledge in sensor construction. The robot hardware was financed from the NEUROS project by the German federal Ministry for Education and Research.

References

- [1] S. Miyazaki, A. Ishida, Capacitive transducer for continuous measurement of vertical foot force, *Med. Biol. Eng. Comp.* 22 (1984) 309–316.
- [2] G. K. GM, K. Rajanna, Tactile sensor based on piezoelectric resonance, *IEEE sensors journal* 4 (5) (2004) 691–697.
- [3] Schaevitz Engineering, Pennsauken, NJ, LVDT and RVDT linear and angular displacement transducer (1987).
- [4] N. Futai, N. Futai, K. Matsumoto, I. Shimoyama, A flexible micromachined planar spiral inductor for use as an artificial tactile mechanoreceptor, *Sensors and Actuators A-Physical* 111 (2-3) (2004) 293–303.
- [5] H. R. Nicholls, M. H. Lee, A survey of robot tactile sensing technology, *International Journal of Robotics Research* 8 (3) (1989) 3–30.
- [6] M. H. Lee, H. R. Nicholls, Tactile sensing for mechatronics - a state of the art survey, *Mechatronics* 9 (1999) 1–31.
- [7] H. Liu, P. Meusel, G. Hirzinger, A tactile sensing system for the DLR three-finger robot hand, in: *Proceedings International Symposium on Measurement and Control in Robotics, 1995*, pp. 91–96.
- [8] J. Paradiso, J. Lifton, M. Broxton, Sensate media - multimodal electronic skins as dense sensor networks, *BT Technology Journal* 22 (4) (2004) 32–44.
- [9] B. Kane, M. Cutkosky, G. Kovacs, A traction stress sensor array for use in high-resolution robotic tactile imaging, *Journal of Microelectromechanical Systems* 9 (4) (2000) 425–434.
- [10] P. Schmidt, E. Maël, R. P. Würtz, European Patent Number: EP 1 142 118 B1 Tastsensor, Europäisches Patentamt, München, patent owner: rubitec GmbH, D-44801 Bochum (2003).
- [11] P. Schmidt, E. Maël, R. P. Würtz, US Patent Number: 6 593 756 Tactile sensor, United States Patent and Trademark Office (2003).
- [12] P. Schmidt, E. Maël, R. P. Würtz, Japanese patent Tactile sensor, submitted (1999).

- [13] P. Schmidt, Aufbau taktiler Sensoren für eine Roboterhand, Tech. Rep. IRINI99-05, Institute for Neurocomputing, Ruhr-University Bochum, D-44780 Bochum (1999).
- [14] M. Becker, E. Kefalea, E. Maël, C. von der Malsburg, M. Pagel, J. Triesch, J. C. Vorbrüggen, R. P. Würtz, S. Zadel, GripSee: A gesture-controlled robot for object perception and manipulation, *Autonomous Robots* 6 (2) (1999) 203–221.
- [15] R. Howe, I. Kao, M. Cutkosky, The sliding of robot fingers under torsion and shear loading, in: *Proceedings of ICRA, Philadelphia, 1988*, pp. 103–108.
- [16] C. Melchiorri, Slip detection and control using tactile and force sensors, *IEEE-ASME Transactions on Mechatronics* 5 (3) (2000) 235–243.
- [17] R. Fearing, Tactile sensing mechanisms, *International Journal of Robotics Research* 9 (3) (1990) 3–23.
- [18] R. Dillmann, Teaching and learning of robot tasks via observation of human performance, *Robotics and Autonomous Systems* 47 (2-3) (2004) 109–116.
- [19] R. Zöllner, O. Rogalla, R. Dillmann, Integration of tactile sensors in a programming by demonstration system., in: *Proceedings of ICRA, 2001*, pp. 2578–2583.
- [20] T. Wösch, W. Feiten, Tactile interaction between human and robot, in: E. Prassler, G. Lawitzky, A. Stopp, G. Grunwald, M. Hägele, R. Dillmann, I. Iossifidis (Eds.), *Advances in Human-Robot Interaction*, Springer, 2005, pp. 23–34.
- [21] O. Kerpa, K. Weiss, H. Wörn, Development of a flexible tactile sensor system for a humanoid robot, in: *Proceedings IEEE/RSJ International Conference on Intelligent Robots and Systems, Las Vegas, 2003*.
- [22] E. Maël, Adaptive and flexible robotics for visual and tactile grasping, Ph.D. thesis, Physics Dept., Univ. of Bochum, Germany (Dec. 2000).
- [23] P. Payeur, C. Pasca, A. Cretu, E. Petriu, Intelligent haptic sensor system for robotic manipulation, *IEEE Trans. Instrumentation and Measurement* 54 (4) (2005) 1583–1592.
- [24] H. Edelsbrunner, E. P. Mücke, Three-dimensional alpha shapes, *ACM Transactions on Graphics* 13 (1) (1994) 43–72.
- [25] P. A. Schmidt, Ein modulares Robotersystem zum Ertasten und Manipulieren von Objekten, Shaker Verlag, Aachen, 2005.
- [26] G. Westphal, R. P. Würtz, Fast object and pose recognition through minimum entropy coding, in: *17th International Conference on Pattern Recognition (ICPR 2004)*, Cambridge, Vol. 3, IEEE Press, 2004, pp. III–53–III–56.
- [27] P. Schmidt, G. Westphal, Object manipulation by integration of visual and tactile representations, in: U. J. Ilg, H. H. Bülthoff, H. A. Mallot (Eds.), *Dynamic Perception*, infix Verlag/IOS press, 2004, pp. 101–106.